Gas-Phase Reactions of H_3Si^- and Me_3Si^-. The Formation of Si-O and Si-S Bonds. A Flowing Afterglow and ab Initio Study

John C. Sheldon,[†] John H. Bowie,*[†] Charles H. DePuy,[‡] and Robert Damrauer[§]

Contribution from the Departments of Chemistry, University of Adelaide, South Australia 5001, University of Colorado, Boulder, Colorado 80309, and University of Colorado at Denver, Denver, Colorado 80202. *Received April 22, 1986*

Abstract: The ions H_3Si^- and Me_3Si^- undergo Si-O and/or Si-S bond forming reactions with CO_2, COS, CS_2, SO_2, N_2O, MeNCO, and MeNCS forming H_3SiO^-, Me_3SiO^-, H_3SiS^-, or Me_3SiS^- ions as appropriate. The rates of these reactions vary markedly, e.g., the reaction of H_3Si^- with CS_2 (to form H_3SiS^- + CS) occurs at every encounter, whereas that of H_3Si^- with N_2O (to form H_3SiO^- plus N_2) occurs for only one in every thousand collisions. Ab initio calculations (at 6-31G level) for the reactions of H_3Si^- with CO_2, CS_2, SO_2, and N_2O suggest different and complex reaction pathways. The reaction of H_3Si^- with CO_2 is characterized by initial approach to carbon, and subsequent rearrangements are required to form H_3SiO^-. H_3SiS^- is formed by a simple path from CS_2 following initial attack at sulfur. H_3Si^- reacts with SO_2 in alternative ways to form five-coordinate intermediate 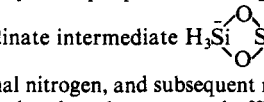 which subsequently decomposes to H_3SiO^- plus SO. H_3Si^- is likely to attack N_2O at the terminal nitrogen, and subsequent rearrangement forms H_3SiO^-. The length, or complexity of the reaction pathway appears inversely related to the measured efficiency in the majority of reactions.

Mechanistic studies of silicon reactions have become increasingly important because of the expanding role of the synthetic utility of this element in the condensed phase.[1] We have carried out mechanistic studies of negative ion-molecule reactions of silicon compounds in the gas phase using the flowing afterglow (FA)[2-6] and ion cyclotron resonance (ICR)[7-10] techniques. Reports of negative ion silicon chemistry include the formation and decomposition of trigonal-bipyramidal silicon species,[2,7-9] comparison of nucleophilic substitution reactions at carbon and silicon,[3,10] and the formation of novel anions by nucleophilic displacement at silicon,[4,5,7] for example, the acetyl anion.[5]

$$Nu^- + Me_3SiSiMe_3 \rightarrow Me_3Si^- + Me_3SiNu \quad (1)$$

$$Me_3Si^- + N_2O \rightarrow Me_3SiO^- + N_2 \quad (2)$$

Little is known of the reactivity of the negative ion H_3Si^- or of its analogoue Me_3Si^-. The acidity of H_4Si has been bracketed at 371.5 kcal mol^{-1},[11] which makes H_3Si^- a base of comparable strength to, for example, H_2P^-.[12] Me_3Si^- may be produced by the reaction between Nu^- (Nu = F, HO, MeO, NH_2) and hexamethyldisilane[6] (eq 1), and the only reaction of the ion which has been described is the unusual oxygen transfer from N_2O shown in eq 2.[6]

In this paper we describe the application of the flowing afterglow technique to investigate reactions of H_3Si^- and Me_3Si^- in which Si-O and Si-S bond formation occurs. Ab initio calculations have been used to probe the mechanisms of the more important of these reactions. An inverse correlation between the complexity and rate of a particular reaction is a general feature of certain of the studied reactions.

Experimental Section

All experiments were performed at 300 K with the flowing afterglow system described previously.[13] Typical helium pressures and flow rates were 0.3 Torr and 14 STP cm^3 s^{-1}. Amide ions were prepared by electron impact on ammonia. Me_3Si^- was prepared by the reaction of NH_2^- on hexamethyldisilane. H_3Si^- was prepared by proton abstraction from silane by NH_2^- [minor products were formed by the following reactions: NH_2^- + SiH_4 → H_3Si-^-NH + H_2 and H_3SiNH + SiH_4 → $(H_3Si)_2N^-$ + H_2]. Neutral reactants were obtained from commercial suppliers, and their flow rates were determined by monitoring the pressure increase with time in a calibrated volume. Rate coefficients are an average of three determinations carried out at different neutral flow rates and are correct to ±10%. Product distributions (branching ratios) were determined as described previously.[14]

Results and Discussion

(A) Flowing Afterglow Experiments. In Table I are recorded the products and rates of the reactions of H_3Si^- and Me_3Si^- with a number of molecules which effect either oxygen of sulfur transfer to silicon. The slowest reaction is that between H_3Si^- and N_2O (efficiency 0.0015, cf. eq 2) and the fastest that of H_3Si^- with CS_2 (efficiency 0.95). In a general sense the rates of H_3Si^- and Me_3Si^- with a particular substrate are of the same order: there is no clear

[†] University of Adelaide.
[‡] University of Colorado, Boulder.
[§] University of Colorado at Denver.

(1) Weber, W. P. *Silicon Reagents for Organic Synthesis*; Springer-Verlag: 1983.
(2) DePuy, C. H.; Bierbaum, V. M.; Flippin, L. A.; Grabowski, J. J.; King, G. K.; Schmitt, R. J.; Sullivan, S. A. *J. Am. Chem. Soc.* **1980**, *102*, 5012. Sullivan, S. A.; DePuy, C. H.; Damrauer, R. *J. Am. Chem. Soc.* **1981**, *103*, 480. Squires, R. R.; DePuy, C. H. *Org. Mass. Spectrom.* **1982**, *17*, 187. DePuy, C. H.; Bierbaum, V. M.; Damrauer, R. *J. Am. Chem. Soc.* **1984**, *106*, 4051.
(3) Damrauer, R.; DePuy, C. H.; Bierbaum, V. M. *Organometallics* **1982**, *1*, 1553.
(4) DePuy, C. H.; Bierbaum, V. M.; Flippin, L. A.; Grabowski, J. J.; King, G. K.; Schmitt, R. J.; Sullivan, S. A. *J. Am. Chem. Soc.* **1983**, *101*, 5012.
(5) DePuy, C. H.; Bierbaum, V. M.; Damrauer, R.; Soderquist, J. A. *J. Am. Chem. Soc.* **1985**, *107*, 3385.
(6) DePuy, C. H.; Damrauer, R. *Organometallics* **1984**, *3*, 362.
(7) Klass, G.; Trenerry, V. C.; Sheldon, J. C.; Bowie, J. H. *Aust. J. Chem.* **1981**, *34*, 519.
(8) Sheldon, J. C.; Hayes, R. N.; Bowie, J. H.; DePuy, C. H. *J. Chem. Soc., Perkin Trans. 2*, in press.
(9) Sheldon, J. C.; Bowie, J. H.; Hayes, R. N. *Nouv. J. Chim.* **1984**, *8*, 79. Hayes, R. N.; Bowie, J. H.; Klass, G. *J. Chem. Soc., Perkin Trans. 2* **1984**, 1167.
(10) Sheldon, J. C.; Hayes, R. N.; Bowie, J. H. *J. Am. Chem. Soc.* **1984**, *106*, 7711.
(11) Bartmess, J. E.; Scott, J. A.; McIver, R. T. *J. Am. Chem. Soc.* **1979**, *101*, 6042.
(12) Anderson, D. R.; DePuy, C. H.; Filley, J.; Bierbaum, V. M. *J. Am. Chem. Soc.* **1984**, *106*, 6513.
(13) Bierbaum, V. M.; DePuy, C. H.; Shapiro, R. H.; Stewart, J. H. *J. Am. Chem. Soc.* **1976**, *98*, 4229.
(14) Anderson, D. R.; DePuy, C. H.; Bierbaum, V. M. *J. Am. Chem. Soc.* **1983**, *105*, 4244.
(15) Su, T.; Bowers, M. T. *Int. J. Mass Spectrom. Ion Phys.* **1973**, *12*, 347.

0002-7863/86/1508-6794$01.50/0

Table I. Products, Branching Ratios, Rate Constants, and Efficiencies of Reactions of H_3Si^- and Me_3Si^- Involving Oxygen or Sulfur Transfer to Silicon

		branching ratio		k_{expt}[a]		k_{expt}/k_{ADO}[b]	
neutral	products	R = H	R = Me	R = H	R = Me	R = H	R = Me
CO_2	$R_3SiO^- + CO$	1.0[c]	1.0[c]	3.4×10^{-10}	8.6×10^{-11}	0.36	0.11
COS	$R_3SiS^- + CO$	1.0	1.0	7.2×10^{-10}	3.1×10^{-10}	0.51	0.28
CS_2	$R_3SiS^- + CS$	1.0	1.0	1.4×10^{-9}	9.2×10^{-10}	0.95	0.80
SO_2	$R_3SiO^- + SO$	1.0[d]	1.0[d]	1.9×10^{-10}	6.0×10^{-10}	0.11	0.43
N_2O	$R_3SiO^- + N_2$	1.0	1.0	1.3×10^{-12}	1.6×10^{-12}	0.0015	0.002
MeNCO	$R_3SiO^- + MeNC$	1.0[e]	1.0[e]	5.1×10^{-10}	3.6×10^{-10}	0.20	0.18
MeNCS	$R_3SiS^- + MeNC$	0.85	0.52	5.2×10^{-10}	6.2×10^{-10}		
	$NCS^- + R_3SiMe$	0.15	0.48	9.2×10^{-11}	5.8×10^{-10}		

[a] In cm^3 molecule $^{-1}$ s^{-1}. [b] Efficiency of reaction. ADO rate calculated by the method of Su and Bowers.[15] [c] At high CO_2 pressure a minor reaction $R_3SiO^- + CO_2 \rightarrow R_3SiOCO_2^-$ is observed. [d] At high SO_2 pressure a minor reaction $R_3SiO^- + SO_2 \rightarrow R_3SiOSO_2^-$ is observed. [e] At high MeNCO pressure a minor reaction $R_3SiO^- + MeNCO \rightarrow Me{-}N{=}C(OSiR_3)O^-$ is observed.

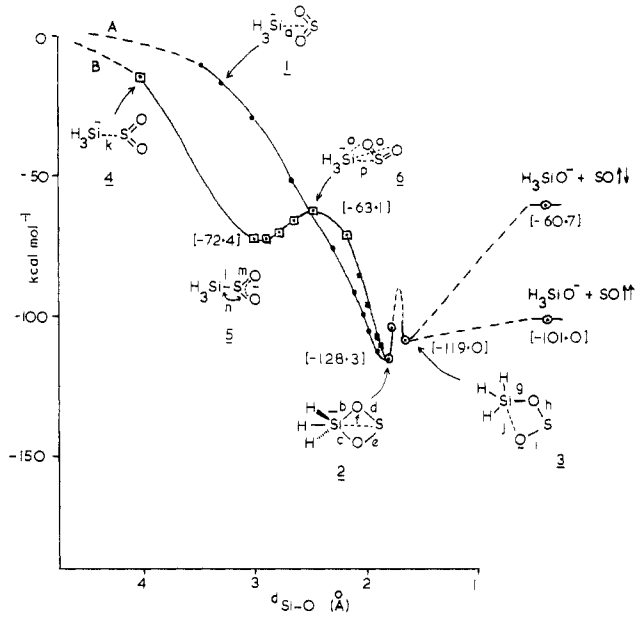

Figure 1. Ab inito calculations (6-31G) for the reaction of H_3Si^- with SO_2. Points ⊙ and ⊡ are fully optimized geometries, and points (●, ■) are obtained from relaxation runs. Geometries (Å, deg) as follows: **1**, $a = 3.15$; **2**, $b = 1.97$, $c = 1.82$, $d = 1.75$, $e = 1.77$, $f = 2.80$; **3**, $g = 1.69$, $h = 1.81$, $i = 1.71$, $j = 3.29$; **4**, $k = 4.0$; **5**, $l = 2.23$, $m = 1.73$, $n = 95$; **6**, $o = 2.39$, $p = 2.22$.

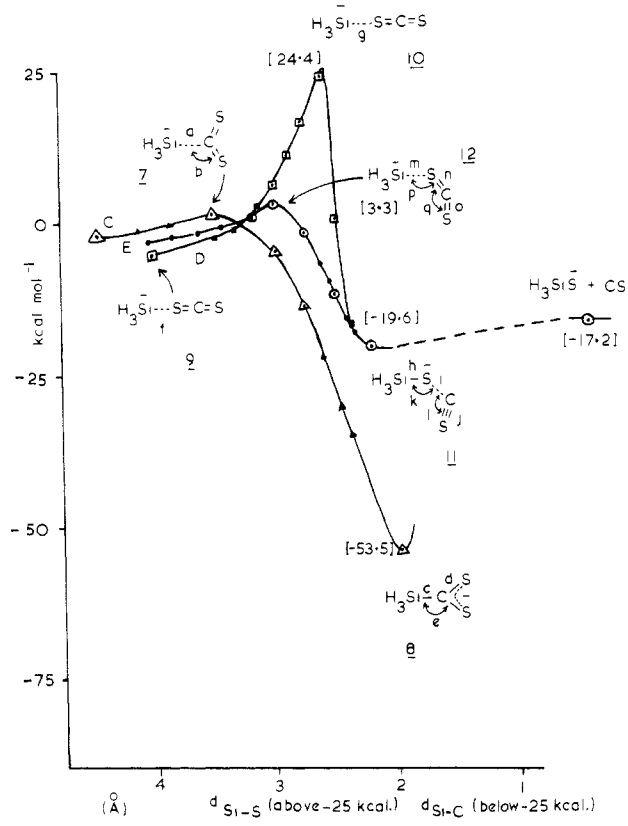

Figure 2. Ab initio calculations (6-31G) for the reaction fo H_3Si^- with CS_2. Points ⊙, ⊡, and ▲ are fully optimized geometries, and points ●, ■, and ▲ are obtained from relaxation runs. Geometries (Å, deg) as follows: **7**, $a = 3.50$, $b = 97$; **8**, $c = 1.92$, $d = 1.73$, $e = 116$; **9**, $f = 4.19$; **10**, $g = 2.65$; **11**, $h = 2.16$, $i = 3.27$, $j = 1.59$, $k = 112$, $l = 106$; **12**, $m = 3.00$, $n = 1.58$, $o = 1.63$, $p = 131$, $q = 166$.

trend shown in Table I in which the reactions of one ion are always faster than the other.

The results listed in Table I raise fundamental problems, both mechanistic and also concerning relative reaction rates. In summary, (i) the rates of the reactions of R_3Si^- (R = H or Me) with CO_2, COS, and CS_2 are in the order $CS_2 > COS > CO_2$.[16] Does the marked difference in rates between CO_2 and CS_2 suggest different mechanisms for the two reactions? For example, do R_3Si^- ions react with CO_2 at carbon (eq 3) and with CS_2 at sulfur (eq 4)?[17] If R_3Si^- ions do react as shown in eq 3, how does the intermediate decompose to products?

$$R_3Si^- + CO_2 \rightarrow [R_3Si{-}CO_2^-] \rightarrow R_3SiO^- + CO \quad (3)$$

$$R_3Si^- + CS_2 \rightarrow [R_3SiS{-}\bar{C}{=}S] \rightarrow R_3SiS^- + CS \quad (4)$$

$$R_3Si^- + N_2O \rightarrow R_3SiN^- + NO \quad (5)$$

Scheme I

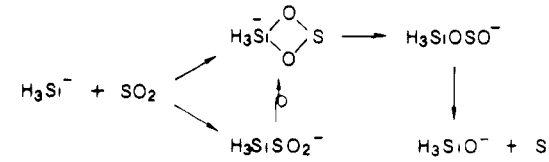

(ii) Do the reactions of R_3Si^- ions with SO_2 occur at sulfur or oxygen, and why do the reactions not occur at every encounter between reactants? (iii) Do the reactions of R_3Si^- ions with N_2O occur at nitrogen or oxygen, and why are these reactions the slowest of all those listed in Table I? In addition, why is the alternative reaction shown in eq 5 not observed? (iv) Five-coordinate silicon negative ions have been proposed as intermediates or products in the majority of silicon reactions that we have studied previously.[2-10] Are such five-coordinate species involved in any of the reactions listed in Table I?

(16) In the case of R_3Si^-/COS reactions, Si–S bond formation is observed, since the formation of CO more than offsets the production of the less thermodynamically stable Si–S bond. ΔH_f for CO is −27.2 kcal mol^{-1} and for CS +64.4 kcal mol^{-1} (Rosenstock, H. M.; Draxl, K.; Steiner, B. W.; Herron, J. T. *J. Phys. Chem. Ref. Data* **1977**, *6*, Suppl. 1). Bond dissociation energy for Si–O is 188 kcal mol^{-1} and for Si–S 148 kcal mol^{-1} (Gaydon *Dissociation Energies and Spectra of Diatomic Molecules*; 3rd ed.; Chapman and Hull: London, 1968).

(17) In the reaction of HO^- with CO_2 and CS_2 the former reaction is thought to take place by attack of HO^- at carbon, the latter at sulfur. Bierbaum, V. M.; Grabowski, J. J.; DePuy, C. H. *J. Phys. Chem.* **1984**, *88*, 1389.

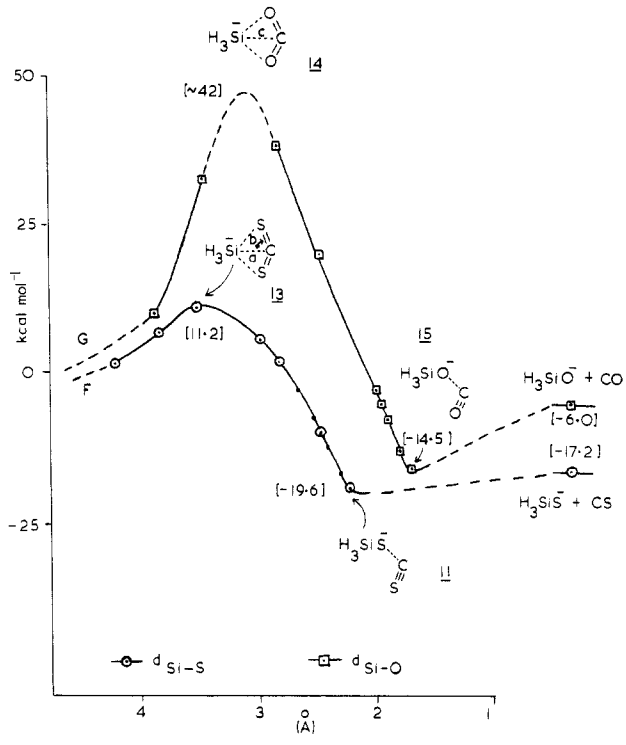

Figure 3. Ab initio calculations (6-31G) for the reactions of H_3Si^- with CS_2 and CO_2 which involve five-coordinate structures. Geometries (Å, deg) as follows: **13**, a = 3.56, b = 70; **14**, c = 3.20. For the geometries of **11** and **15** see Figures 2 and 4.

We have carried out ab initio studies for the reactions of H_3Si^- with SO_2, CS_2, CO_2, and N_2O in order to seek answers to the questions posed above. We will show that the mechanisms can be complex and that each of the four systems studied behaves quite differently.

(B) Ab Initio Studies. Ab initio calculations shown in Figures 1–6 were carried out at the 6-31G level with GAUSSIAN 82.[18] The procedures and strategies used in these calculations have been outlined elsewhere.[10,19,20] Absolute energies of reactants, transition states, and products shown in Figures 1–6 are listed in Table II. The majority of these species have also been calculated at the 6-31^{++}G level; comparisons of 6-31G and 6-31^{++}G energies are made in Table II.[20]

(1) The H_3Si^-/SO_2 Reaction. We have investigated the approach of H_3Si^- along the C_{2v} axis of SO_2 and find that different adducts are formed depending on whether the approach is on the oxygen or sulfur side of the v-shaped molecule. These reactions are designated A and B respectively in Figure 1. There are no significant barriers along either route. Addition from the oxygen side of the molecule proceeds through **1** to the pentacoordinate intermediate **2**. Direct addition of H_3Si^- to sulfur proceeds through **4** to the tetrahedral silicon intermediate **5**. The two intermediates **2** and **5** interconvert over a modest barrier by the simple motion of the SO_2 group rolling onto its other side relative to H_3Si^-.

Scheme II

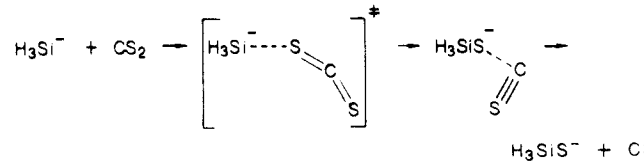

Scheme III

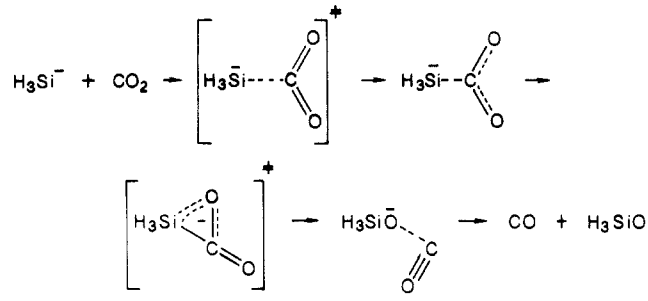

Intermediate **2** ring opens to **3**[21] which subsequently eliminates SO.[22] Depending on the spin state of SO, the reaction is exothermic by either 60.7 or 101.0 kcal mol^{-1} (6-31G). Ab initio calculations therefore suggest the mechanistic pathway summarized in Scheme I.

(2) The H_3Si^-/CS_2 Reaction. The H_3Si^- ion may approach the carbon disulfide molecule toward either carbon or sulfur. The approach of H_3Si^- toward carbon along a twofold axis of CS_2 (channel C, Figure 2) proceeds to transition state **7**; thereafter H_3Si^- relaxes strongly onto carbon yielding **8**. We believe that **8** is not an intermediate in the formation of H_3SiS^-, since (i) a stable species **8** is not observed in the flowing afterglow reaction and (ii) its conversion into some Si–S species involves a prohibitive endothermic barrier.[23]

We have also examined the approach of H_3Si^- directly toward a single sulfur atom. The colinear orientation is shown in Figure 2 as route D. A weak association complex **9** is formed; the reaction proceeds through transition state **10** to association complex **11** which decomposes to products. The reaction is exothermic [-17.2 kcal mol^{-1} (6-31G)], but the barrier of 24.4 kcal mol^{-1} to transition state **10** is too high for the process to occur under the flowing afterglow conditions.[24] Approach of H_3Si^- at an angle of 120° to the CS_2 axis is shown in Figure 2 as route E; this we suggest is the preferred reaction path. This pathway goes through a minor barrier [3.3 kcal mol^{-1} (6-31G)] to transition state **12** which is followed by direct relaxation into products H_3SiS^- and CS. In this reaction the developing Si–S bond changes the linear arrangement of CS_2 into one which is bent, and this causes the remaining sulfur to swing closer to silicon. No discrete pentacoordinate silicon species is formed; instead, motion continues with separation of CS. This concerted bending and bond breaking seems characteristics of attack of H_3Si^- on linear triatomics. The

(18) Binkley, J. S.; Frisch, M. J.; DeFrees, D. J.; Raghavachari, K.; Whiteside, R. A.; Shlegel, H. B.; Fluder, E. M.; Pople, J. A. Gaussian 82, Carnegie Mellon University.

(19) Sheldon, J. C.; Currie, G. J.; Lahnstein, J.; Hayes, R. N.; Bowie, J. H. *Nouv. J. Chim.* **1985**, *9*, 205.

(20) We find that addition at low exponent functions (diffuse functions) makes a significant difference to the structures and energies of negative ion systems when the site of the negative charge involves hydrogen atoms in some way (say, as H^- or in hydrogen bonding). When the site of the negative charge is on some other atom (as in the present study) the addition of low exponent functions makes no significant difference. A comparison of 6-31G and 6-31^{++}G (includes diffuse functions) energies of 24 structures shown in Table II indicates energy differences from 0 to 8 kcal mol^{-1} with a mean value of 2.8 kcal mol^{-1}. In addition, we find that region of Figure 4 in the vicinity of $H_3Si^-\cdots CO_2$ (**16**) to the formation of $H_3SiCO_2^-$ (**18**) is very similar at 6-31G and 6-31^{++}G. The energy and bond distances given for **16** (Figure 4) should be compared with the following values obtained at 6-31^{++}G; (**16**) E = −5.5 kcal mol^{-1}, a = 1.56, b = 3.48, c = 1.16, d = 117.4, e = 121.3, f = 96.0.

(21) Ab initio calculations (6-31G) indicaate a second "stable" conformer

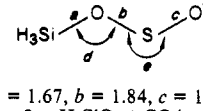

E = −113.0 kcal mol^{-1}; a = 1.67, b = 1.84, c = 1.69, d = 131, and e = 107.

(22) The interconversion **3** to H_3SiO^- + SO involves the cleavage of a Si–O bond for which there will be a small barrier. This barrier was not calculated since our single determinant wave functions cannot describe the change in spin in the system with the emergence of triplet SO.

(23) Ab initio calculations show that a roll-over mechanism similar to **2** → **5** (Figure 1) has a barrier of some 50 kcal mol^{-1} in this case. We were surprised both with the observation that **8** is not observed experimentally and that there is no low-energy pathway from **8** to H_3SiS^-. Presumably, if **8** is formed, it must be unstable under the experimental conditions used and revert to reactants.

(24) Since flowing afterglow experiments are carried out in helium buffer gas at ca. 0.3 Torr, the majority of the excess energy of reactant ions will be removed by collisions with helium.

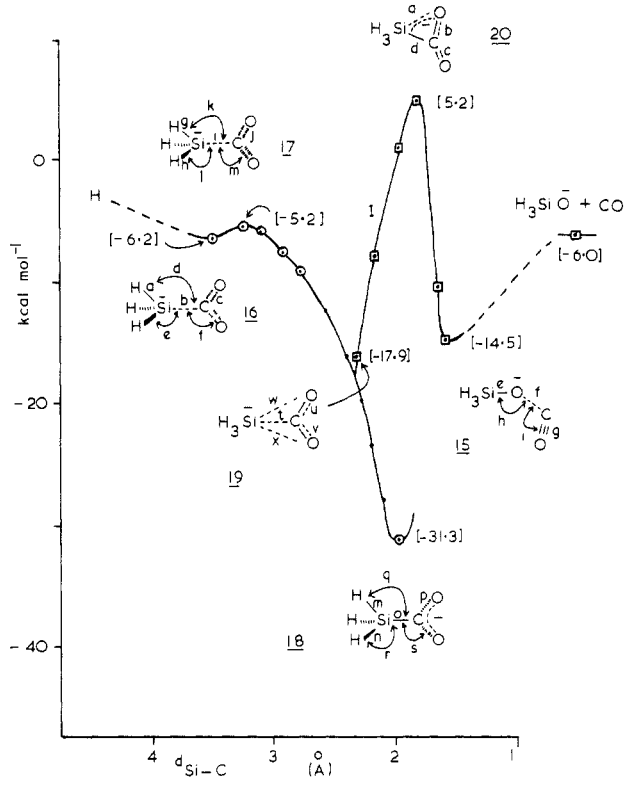

Figure 4. Ab initio calculations (6-31G) for the reaction of H_3Si^- with CO_2. Geometries (Å, deg) as follows: **16**, a = 1.56, b = 3.52, c = 1.16, d = 118, e = 122, f = 95; **17**, g = 1.56, h = 1.56, i = 3.20, j = 1.17, k = 119, l = 121, m = 98; **18**, m = 1.51, n = 1.50, o = 1.97, p = 1.26, q = 110.8, r = 113.8, s = 115.1; **19**, t = 1.89, u = 1.27, v = 1.20, w = 2.30, x = 2.92; **20**, a = 1.80, b = 1.36, c = 1.22, d = 1.94; **15**, e = 1.64, f = 2.40, g = 1.14, h = 158, i = 99.

reaction sequence shown in Scheme II is thus supported by ab initio calculations.

The reaction of H_3Si^- with SO_2 proceeds through the intermediacy of a five-coordinate intermediate (**2**, Figure)1. We were interested to determine whether a similar pathway can occur in the case of CS_2 (and CO_2, see below). The results are shown in Figure 3. The reaction can occur (channel F, Figure 3) but the high barrier to transition state **14** precludes its operation in the flowing afterglow experiment. It is the energy required to bend the linear carbon disulfide molecule that makes this pathway unfavorable.

(3) The H_3Si^-/CO_2 Reaction. Direct approach of H_3Si^- toward an oxygen of CO_2 from any direction (cf. routes D and E for CS_2, Figure 2) is calculated to be repulsive and will not occur under the experimental conditions used. Formation of a pentacoordinate intermediate (channel G, Figure 3) is theoretically possible, but again the high barrier precludes the operation of such a process under the conditions used in the flowing afterglow experiment. We conclude that the formation of H_3SiO^- from CO_2 must therefore involve the initial approach of H_3Si^- toward carbon.

Channel H in Figure 4 shows approach of H_3Si^- toward the carbon of carbon dioxide, proceeding through **16** and **17** after which there is steeply descending channel to $H_3SiCO_2^-$ (**18**). This ion is not observed in the reaction; how can it rearrange to H_3SiO^- and carbon monoxide? Any direct rearrangement which involves concomitant Si–C bond rupture and Si–O bond formation has an unacceptably large barrier and is not a possibility. Thus we have undertaken an exhaustive search for a crossover point on channel H which will lead directly to the required products. This is shown in Figure 4, and the lowest energy pathway is designated channel I. The "roll-over" mechanism proceeds through **19** to transition state **20** which then relaxes through **15** to products. The reaction is exothermic by 6 kcal mol^{-1}, and the estimated energy of transition state **20** is +5.2 kcal mol^{-1}. The predicted mechanism is summarized in Scheme III.

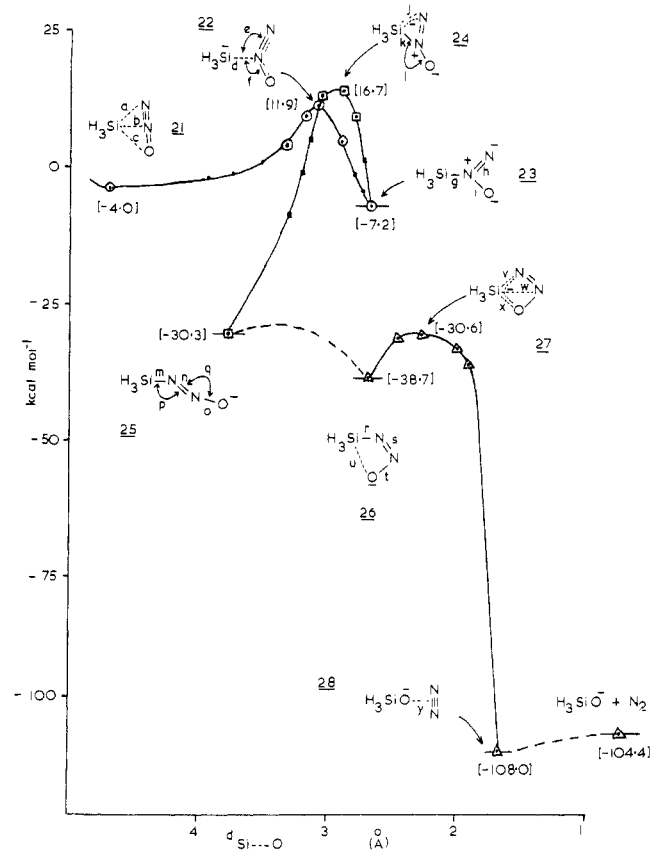

Figure 5. Ab initio calculations (6-31G) for the reaction of H_3Si^- at the central nitrogen of N_2O. Geometries (Å, deg) as follows: **21**, a = 3.97, b = 4.12,f c = 4.64; **22**, b = 2.50, e = 120, f = 107; **23**, g = 1.84, h = 1.22, i = 1.39; **24**, j = 2.20, k = 1.775, l = 138; **25**, m = 1.77, n = 1.29, o = 1.26, p = 114, q = 117; **26**, r = 1.83, s = 1.26, t = 1.29, u = 2.68; **27**, v = 1.91, w = 2.51, x = 1.99; **28**, y = 2.93.

(4) The H_3Si^-/N_2O Reaction. A search of various approaches of the H_3Si^- ion toward N_2O establishes that there is a strong repulsion from the oxygen end and significant repulsion from the terminal nitrogen of N_2O. This is evidenced (i) by the fact that the long-range potential minima (corresponding to van der Waals contact between the two molecules) is at abnormally long separations, i.e., 8.5 Å for Si to central N attachment and 6 Å for the linear arrangements H_3Si^----ONN and H_3Si^----NNO; and ii), because the most stable association complex of H_3Si^- and N_2O involves a somewhat broadside arrangement of N_2O in which silicon is about 4 Å from each nitrogen. *If these long range interactions play a directive role, we may expect there to be a higher probability of attack of H_3Si^- on either nitrogen rather than on oxygen.* Let us nevertheless consider the reactions which may occur when H_3Si^- reacts at each center in N_2O.

In Figure 5 we show the reactions which occur when H_3Si^- approaches toward the central nitrogen of N_2O, and in Figure 6 we consider the reactions which occur when H_3Si^- approaches (i) the terminal nitrogen at an angle close to 120° to the N–N bond (trajectory J) and (ii) the oxygen at an angle close to 120° to the N–O bond (trajectory K). This is the most complex of the four systems we have studied because, theoretically, it is possible to produce the desired products by attack of H_3Si^- at any one of the three atoms of N_2O, i.e., there are (at least) three competitive pathways to products H_3SiO^- and N_2.

Consider first the data in Figure 5. The ion H_3Si^- approaches the central nitrogen of N_2O to form association complex **21**. The reaction then goes through transition state **22** on the way to **23**. No ions corresponding to (H_3Si^- + N_2O) are observed in the flowing afterglow experiment. Intermediate **23** may dissociate to reactants, or alternatively reaction may continue through transition state **24** to the ring opened structure H_3Si—N=NO$^-$ (**25**). Rearrangements **25** → **26** → **27** → **28** finally produce

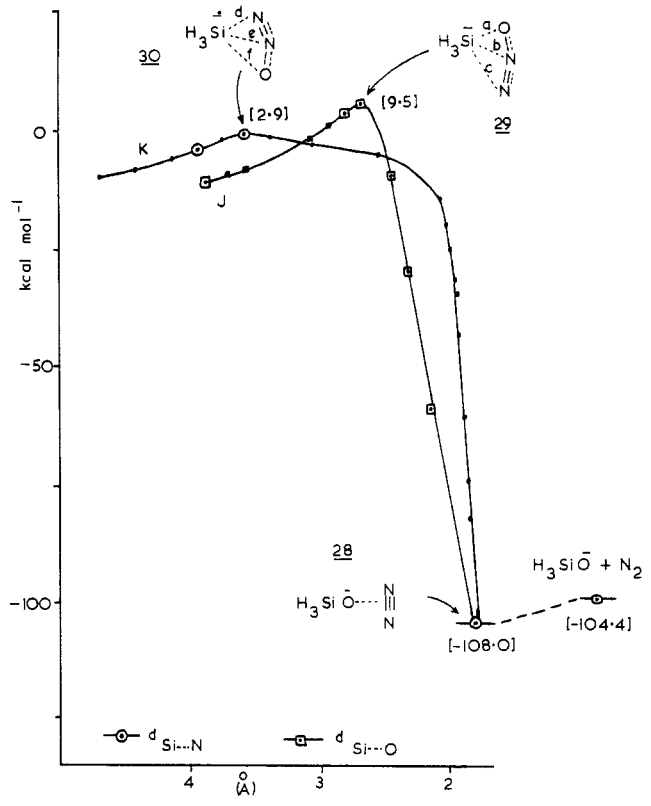

Figure 6. Ab inito calculations (6-31G) for the reactions of H_3Si^- with the oxygen and the terminal nitrogen of N_2O. Geometries (Å, deg) as follows: **29**, a = 2.80, b = 3.19, c = 3.74; **30**, d = 2.80, e = 3.28, f = 3.56.

H_3SiO^- and nitrogen. There are two bottlenecks in this reaction sequence, since the two transition states **22** and **24** have energies of +11.9 and +16.7 kcal mol^{-1} with respect to reactants (considered to be zero).

In contrast, the two reaction sequences shown in Figure 6 are more straightforward. Plot J shows the approach of H_3Si^- toward oxygen: there is a barrier of 9.5 kcal mol^{-1} to transition state **29** and then a steep channel to solvated ion **28** which immediately decomposes to products. This reaction is directly comparable to channel E (Figure 2) in the CS_2 system. In the alternative reaction K, H_3Si^- approaches the terminal nitrogen, there is then a modest barrier (2.9 kcal mol^{-1}) to transition state **30**, and then a facile rearrangement in the descending channel forms **28**.[25] If we consider the avaialble evidence, viz., (i) long-range interactions indicate a higher probability of H_3Si^- reacting at either nitrogen rather than at oxygen and (ii) the barriers to the reactions shown in Figure 5 are higher than that for reaction J (Figure 6), which in turn is higher than that calculated for reaction K, we must conclude that *K represents the most probable mechanism under the experimental conditions operating.* This mechanism is summarized in Scheme IV.

(C) The Correlation between Mechanism and Rate. It has been known for some time that not all exothermic gas-phase ion–molecule reactions proceed at the collision rate.[26,27] Brauman[28] and Kebarle[29] have shown how density of state arguments may be used to rationalize slow rates of certain simple gas-phase

Scheme IV

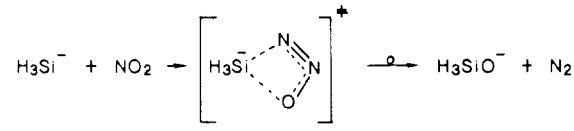

reactions in which a transition state is slightly less negative in energy than reactants. Yet the situation is clearly more complex than this: we really need to know the potential surface for the reaction. In very simple terms once an orbiting complex is formed there will be a certain probability of the complex entering the reaction channel (even in the absence of an activation barrier). Second, once an intermediate has been formmd (even one with significant negative energy of formation) there is a finite probability of the appropriate exit channel being found.[30] Therefore in the general case of an exothermic ion molecule reaction in which there are a number of transition states and intermediates, even when these are all more negative in energy than reactants, there is a likelihood that the rate will decrease as the complexity of the reaction (number of intermediates) increases.[31]

The situation is clearly complex for the four systems described in detail above since (i) several reaction channels are available for three of the four systems and (ii) in three cases ab initio calculations indicate transition state marginally more positive in energy than reactants, viz., +3.3, +5.2, and +2.9 kcal mol^{-1} (6-31G) in Figures 2, 4, and 6, respectively. Reactant ions undergo collisions with the helium buffer gas in flowing afterglow experiments, and energetic species will be substantially deactivated. Some ions could nevertheless still have sufficient vibrational (and rotational) energy to surmount the modest barriers listed above.[32]

Qualitative correlations between rates and mechanism can be made for a number of the studied systems. The SO_2 reactions have moderate rates [efficiencies 0.11 and 0.43 for H_3Si^- and Me_3Si (Table I)]. Figure 1 shows two reaction channels with two and three intermediates, respectively, thus rates slower than the collision frequency are not unexpected. The relative rates of the CS_2 and CO_2 reactions are significantly different, with CS_2 reactions occurring at virtually every encounter between reactants. This must mean (i) that the Si–S interaction shown in Figure 2 (channel E) occurs at every encounter between reactants, (ii) that the small barrier (3.3 kcal mol^{-1}) is readily surmounted, and (iii) that entropy differences[28] between reactants and transition state must be small. The barrier for the CO_2 reaction (Figure 4) is

(25) Close approach of the silicon toward the terminal nitrogen induces the usual bending in the triatomic, resulting in the close approach of oxygen toward silicon with the ultimate formation of H_3SiO^- and N_2.

(26) Tanaka, K.; Mackay, G. I.; Payzant, J. D.; Bohme, D. K. *Can. J. Chem.* **1976**, *54*, 1643. Bohme, D. K.; Young, L. B. *J. Am. Chem. Soc.* **1970**, *92*, 7354. Bohme, D. K.; Mackay, G. I.; Payzant, J. D. *J. Am. Chem. Soc.* **1974**, *96*, 4027.

(27) Asubiojo, O. I.; Brauman, J. I. *J. Am. Chem. Soc.* **1979**, *101*, 3715.

(28) Olmstead, W. N.; Brauman, J. I. *J. Am. Chem. Soc.* **1977**, *99*, 4219. Pellerite, M. J.; Brauman, J. I. *J. Am. Chem. Soc.* **1980**, *102*, 5993.

(29) Caldwell, G.; Magnera, T. F.; Kebarle, P. *J. Am. Chem. Soc.* **1984**, *106*, 959.

(30) A strongly bound intermediate can be viewed as a deep well in the system's potential energy hypersurface. A molecular system resulting from a gas-phase association enters such a well with excess energy and so traverses its upper levels repeatedly by undergoing a series of reflections on the upper walls. The oscillating system eventually finds and passes through one of the several gaps (channels) in the well's rim and moves on to another molecular configuration. The freedom of an intermediate to exit by chance either a reaction channel or back into the original entry channel is equivalent to the usual notion of reversibility of reaction or equilibrium.

(31) (i) For example, if we have a reaction involving three reactive intermediates in which the first intermediate is formed at every collision, but the probability of exit from each intermediate is 50%, the overall efficiency of the reaction will be 0.25. (ii) It must be stressed that not all complex reactions have rates lower than the collision rate. For example, the reaction $MeO^-\cdots HOMe + MeCOMe \rightarrow CH_2{=}CH(Me){-}O^-\cdots HOMe + MeOH$ is one in which it is proposed that there are three reactive intermediates and for which the overall efficiency is 0.93 (Bowie, J. H.; Hayes, R. N.; Sheldon, J. C.; DePuy, C. H. *Aust. J. Chem.*, in press).

(32) There are two ways to explain why reactions with calculated endothermic barriers of up to 5 kcal mol^{-1} occur under flowing afterglow conditions: (i) even though the excess energy of reactant ions is substantially removed by collisions with helium buffer gas, some ions may still have some vibrational energy. If this is so that energy might be as high as 6 kcal mol^{-1} (the vibrational mode of H–Si is equivalent to ca. 6 kcal mol^{-1}: Stewart, A.; Nielsen, P. *J. Chem. Phys.* **1934**, *2*, 712; *Phys. Rev.* **1935**, *47*, 828). (ii) A reviewer has suggested that our calculated value of an endothermic barrier of say 5 kcal mol^{-1} may indeed be close to thermoneutral if even higher level calculations were used (for example, it can be seen in Table II that in individual cases energies become more negative in going from 6-31G to 6-31^{++}G). The reviewer may be right, but we must stress that in constructing a reaction coordinate profile we are considering relative energies, and individual differences will certainly cancel to some extent. On the other hand, the other source of error in these calculations is the absence of correlation correction. This might lower the overall energy profile by say 5 kcal mol^{-1}.

Table II. Absolute Energies (au) (and AE in kcal mol^{-1}, where appropriate) for Species Shown in Figures 1–6.

species	6-31G//6-31G (AE)	6-31⁺⁺G//6-31G (AE)	6-31⁺⁺G//6-31⁺⁺G (AE)
H_3Si^-	−290.574 11		−290.583 25
H_3SiO^-	−365.431 31		−365.448 67
H_3SiS^-	−688.150 82		−688.158 97
SO_2	−546.938 61		−546.946 47
CS_2	−832.789 65		−832.792 18
CO_2	−187.514 95		−187.519 43
N_2O	−183.558 62		−183.565 64
SO (singlet)	−472.242 60		
SO (triplet)	−472.178 00		−472.247 20
CS	−435.240 43		−435.243 88
CO	−122.667 22		−112.671 51
N_2	−108.868 00		−108.871 79
2	−837.717 43 (−129)	−837.732 17 (−127)	−837.733 82 (−128)
3	−837.702 23 (−119)	−837.727 83 (−124)	
5	−837.628 16 (−72)	−837.657 80 (−80)	
6	−837.613 73 (−63)	−837.626 66 (−61)	
$H_3SiO^- + SO\uparrow\uparrow$	−837.673 91 (−101)		−837.695 87 (−104)
7	−1123.361 71 (1)		
8	−1123.460 87 (−54)	−1123.471 48 (−60)	
10	−1123.327 78 (22)		
11	−1123.394 00 (−19)	−1123.404 46 (−18)	
12	−1123.358 49 (3)		−1123.369 26 (4)
13	−1123.345 58 (11)		
$H_3SiS^- + CS$	−1123.363 76 (−17)		−1123.402 85 (−17)
15	−478.112 30 (−15)	−478.132 62 (−19)	
16	−478.099 11 (−6)		−478.111 36 (−5)
17	−478.098 20 (−6)		−478.111 22 (−5)
18	−478.130 03 (−26)		−478.152 04 (−31)
19	−478.113 20 (−8)		
20	−478.079 21 (6)	−478.097 40 (3)	
21	−474.139 24 (−4)	−474.154 63 (−4)	
22	−474.114 26 (12)		−474.136 22 (8)
23	−474.143 39 (−7)	−474.169 02 (−13)	
24	−474.109 43 (61)		
25	−474.180 95 (−30)	−474.203 59 (−34)	
26	−474.194 60 (−39)	−474.212 76 (−40)	
27	−474.183 71 (−31)		−474.200 23 (−32)
28	−474.304 76 (−108)	−474.325 91 (−111)	
29	−474.117 69 (10)		−474.134 08 (9)
30	−474.128 37 (3)		−474.144 51 (3)
$H_3SiO^- + N_2$	−474.299 31 (−104)		−474.320 46 (−108)

larger than that of the CS_2 reaction. In addition, there are more intermediates in the CO_2 reaction, thus the rates are likely to be slower than those of CS_2 reactions, as observed.

$$R_3Si^- + MeNCO \rightarrow R_3SiO^- + MeNC \quad (6)$$

$$R_3Si^- + MeNCS \rightarrow R_3SiS^- + MeNC \quad (7)$$

The R_3Si^-/MeNCO and R_3Si^-/MeNCS reactions (listed in Table I) are shown in eq 6 and 7, respectively. These processes have moderate rates with R_3SiS^- formation being marginally faster than that of R_3SiO^-. Ab initio calculations have not been performed on these systems: we expect the mechanisms to have features in common with the CS_2 and CO_2 reactions, e.g., R_3Si^- probably reacts with MeNCO at carbon and with MeNCS at sulfur.[33]

Finally, the N_2O reactions are different from all others considered above in that only approximately one in a thousand encounters between reactants leads to products. The slowness of these reactions cannot be explained in terms of the number of intermediates in, or complexity of, the reaction pathways. We conclude that this is an example of a situation where the probability of the initial orbiting complex being able to find entry into the reaction channel K (Figure 6) is low.[34]

In conclusion, the questions raised by the flow afterglow experiments have been answered by the ab initio studies in the following way: (i) The varying rates of CO_2 and CS_2 reactions are due to a more complex mechanistic pathway in the former case: R_3Si^- ions react with the carbon of carbon dioxide and with carbon disulfide at sulfur to ultimately form R_3SiO^- and R_3SiS^-, respectively. (ii) The channels forming R_3SiO^- from SO_2 proceed through a decomposing five-coordinate intermediate in which both oxygens are bound to silicon. Similar intermediates (or in some cases transition states) may be formed for the other systems studied, but high barriers to these structures preclude their formation under the conditions used in flowing afterglow experiments. (iii) R_3Si^- ions may react with N_2O through any atom to form R_3SiO^-, but ab initio calculations suggest that reaction through

(33) (i) A competitive S_N2 reaction occurs between R_3Si^- ions and MeNCS, i.e., $R_3Si^- + MeNCS \rightarrow R_3SiMe + NCS^-$. The corresponding reaction is not observed with MeNCO since NCO^- is a poorer leaving group than NCS^-. (ii) Reaction between R_3Si^- and MeSCN does not form R_3SiN^- ions. Instead the following reactions are observed:

$$R_3Si^- + MeSCN \rightarrow CN^- + R_3SiMe \quad (8)$$

$$R_3Si^- + MeSCN \rightarrow NCS^- + R_3SiMe \quad (9)$$

[H_3Si^-, branching ratios 0.99 (8), 0.01 (9), rates 3.1×10^{-9} cm^3 $molecule^{-1}s^{-1}$ (8) and 3.1×10^{-11} (9); Me_3Si^-, branching ratios 0.98 (8), 0.02 (9), rates 2.4×10^{-9} (8) and 4.8×10^{-11} (9)]. Reaction 8 must involve direct attack of R_3Si^- at sulfur; reaction 9 is an S_N2 process.

(34) (i) The orbiting complex is most likely to relax into the attack of the nucleophile on the central nitrogen atom as has been explained (see Figures 5 and 6). Therefore there is a low probability of the system proceeding into reaction channel K (Figure 6). (ii) A recent general survey of the reactions of nucleophilies with N_2O has shown that such reactions are slow, except in the case of powerful bases, e.g., NH_2^- (Kass, S.; DePuy, C. H. *J. Am. Chem. Soc.*, in press). (iii) A reviewer has suggested that spin barriers may explain the lack of reactivity with N_2O (Armentrout, P. B.; Halle, L. F.; Beauchamp, J. L. *J. Chem. Phys.* **1982**, *76*, 2449). We cannot totally exclude this possibility, but since there is no barrier as such in this reaction to identify as a "spin barrier" it seems unlikely.

the terminal nitrogen is the lowest energy pathway. The very slow rate of these reactions may be due to the low probability of the orbiting complex being able to enter the appropriate reaction channel.

Acknowledgments. The flowing afterglow experiments were carried out while one of us (J. H. Bowie) was on leave at the University of Colorado, Boulder. C. H. DePuy and R. Damrauer acknowledge the support of this work by N.S.F. Grants CHE-8503505 and CHE 83-13826, respectively. We thank the University of Adelaide Computing Centre for facilities.

Registry No. H_3Si^-, 15807-96-2; Me_3Si^-, 54711-92-1; CO_2, 124-38-9; COS, 463-58-1; CS_2, 75-15-0; SO_2, 7446-09-5; N_2O, 10024-97-2; MeNCO, 624-83-9; MeNCS, 556-61-6; H_3SiO^-, 43336-62-5; Me_3SiO^-, 41866-81-3; H_3SiS^-, 81429-19-8; Me_3SiS^-, 88657-58-3; H_3SiOSO, 104114-30-9; O_2, 7782-44-7; S, 7704-34-9; Si, 7440-21-3; $H_3SiCS_2^-$, 104092-12-8; $H_3SiCO_2^-$, 40058-48-8.

Communications to the Editor

Bridging of Macrocycles to Bicycles. New Synthetic Technology for the Construction of Cis- and Trans-Fused Oxopolycyclic Systems

K. C. Nicolaou,* C.-K. Hwang, M. E. Duggan, K. Bal Reddy, B. E. Marron, and D. G. McGarry

Department of Chemistry, University of Pennsylvania Philadelphia, Pennsylvania 19104

Received April 4, 1986

Cis- and trans-fused oxobicyclic and oxopolycyclic systems of type A (Scheme I) are becoming increasingly recognized as common structural features of marine and other natural products such as brevetoxins[1] (trans fusions) and halohydrins[2] (trans and cis fusions). A potentially efficient and economical retrosynthetic disconnection of the bicyclic system A would be the indicated rupture of the central C–C bond, suggesting the macrocycle B (Scheme I) as a precursor, since in the synthetic direction the construction of one bond would result in the simultaneous generation of two rings.[3] Based on this concept, a method for bridging macrocycles of type B that would allow stereoselective entry into both the cis- and trans-fused systems A was sought. Due to the relatively low reduction potential of the C=S bond[4] and the synthetic potential of sulfur for further chemical transformations, macrodithionolactones were chosen as starting materials. Our general strategy for bridging macrocycles to bicycles is depicted in Scheme I. Thus, it was anticipated that electron transfer to a thiocarbonyl group of the macrodithionolide system I would generate a radical anion (II), initiating a sequence leading to a bridged product (IV) as outlined in Scheme I. Quenching of the resulting dianion IV with an electrophile such as MeI was then expected to lead to a stable disulfide (V) which could be chemically manipulated[3b] to a variety of systems including the olefinic compounds VI and the cis- and trans-fused polycycles A (Scheme I).

As a model of the brevetoxin framework, the systems depicted in Scheme II were chosen to test these ideas. Thus, two enantiomeric hydroxy acids in the form of their benzyl derivatives **1a** and **1b** were synthesized[5] and utilized to construct the meso diolide

Scheme I[a]

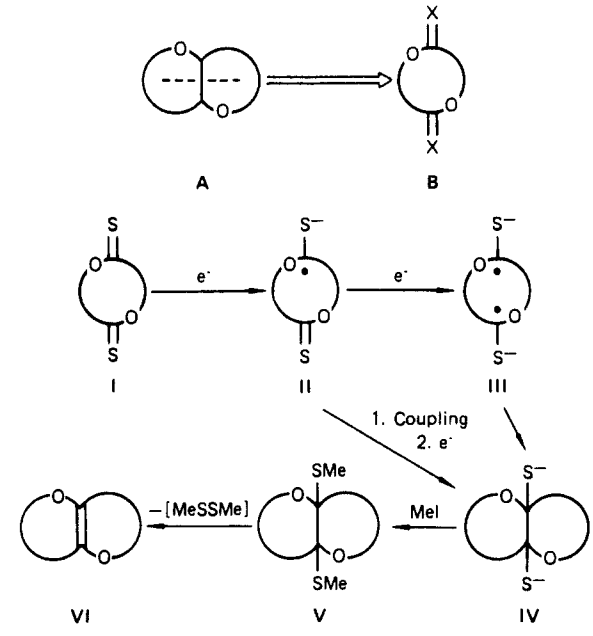

[a] General concept for bridging macrocycles to bicycles by free radical coupling reactions.

2 (C_1 symmetry, esterification followed by debenzylation and macrolactonization[6]) which was then converted to the dithionolide **3** by Lawesson's reagent.[7] When **3** was exposed to sodium naphthalide in THF at −78 °C followed by quenching with CH_3I, the cis-bridged tetracycle **4**[8] (racemic mixture) was isolated as a major product. Dreiding molecular models suggest the syn relationship for the thiocarbonyl groups in **3** rather than the anti arrangement as the preferred conformation and hence this stereochemical outcome was not unexpected. Treatment of the disulfide **4** with *n*-Bu_3SnH in the presence of AIBN resulted in its high-yield conversion to the olefinic compound **5** (meso, C_i symmetry), the ORTEP drawing[9] of which is shown in Scheme II. Photolysis (Hanovia, UV quartz lamp. toluene) of **4** also led to the same product (**5**) in high yield. To enhance the usefulness

(1) Brevetoxin, A: Shimizu, Y.; Chou, H.-N.; Bando, H.; VanDuyne, G.; Clardy, J. C. *J. Am. Chem. Soc.* **1986**, *108*, 514. Brevetoxin B: Lin, Y. Y.; Risk, M.; Ray, S. M.; VanEngen, D.; Clardy, J.; Golik, J.; James, J. C.; Nakanishi, K. *J. Am. Chem. Soc.* **1981**, *103*, 6773.

(2) Uemura, D.; Takahashi, K.; Yamamoto, T.; Katayama, C.; Tanaka, J.; Okumura, Y.; Hirata, Y., *J. Am. Chem. Soc.* **1985**, *107*, 4796. Hirata, Y.; Uemura, D. *Pure Appl. Chem.* **1986**, *58*, 701.

(3) For our recent stepwise entries into oxo rings via C–O bond forming reactions, see (a) tetrahydropyrans: Nicolaou, K. C.; Duggan, M. E.; Hwang, C.-K.; Somers, P. K. *J. Chem. Soc., Chem. Commun.* **1985**, 1359. And oxocenes (b): Nicolaou, K. C.; Duggan, M. E.; Hwang, C.-K. *J. Am. Chem. Soc.* **1986**, *108*, 2468.

(4) Ohno, A. In *Organic Chemistry of Sulfur*; Oae, S., Ed.; Plenum Press: New York, 1977; Chapter 5, pp 189.

(5) These and the other compounds utilized to prepare the macrodithionolides shown in Table I were synthesized by standard methods either as described in ref 3a or from glucal triacetate.

(6) Corey, E. J.; Nicolaou, K. C. *J. Am. Chem. Soc.* **1974**, *96*, 5614.

(7) Pedersen, B. S.; Scheibye, S.; Nilsson, N. H.; Lawesson, S.-O. *Bull. Soc. Chim. Belg.* **1978**, *87*, 223. See also: Cava, M. P.; Levinson, M. I. *Tetrahedron* **1985**, *41*, 5087.

(8) The presence of two thiomethyl signals (250 MHz, $CDCl_3$, δ 2.03, 1.89) in the ^1H NMR spectrum of **4** proved the cis arrangement of the generated bridge. The ^1H NMR spectrum of **4** also showed the signal corresponding to the proton across the oxygen bridge and syn to the thiomethyl group at relatively low field (δ 4.21, ddd, J = 10.0, 10.0, 5.0 Hz). These observations were consistent and assisted in the tentative assignment of stereochemistry in the examples shown in Table I.

(9) We are indebted to Dr. Patrick J. Carrol of this department for solving this X-ray structure.

0002-7863/86/1508-6800$01.50/0